OLI/Landsat-8 semi-analytical based model for retrieving Secchi disk depth in Nova Avanhandava Reservoir

Thanan Rodrigues [1]
Enner Alcântara [2]
Fernanda Watanabe [1]
Luiz Rotta [1]
Nilton Imai [1]

[1] Departamento de Cartografia, Universidade Estadual Paulista – Unesp/FCT
Rua Roberto Símonsen, 305 - 19060-900 - Presidente Prudente, SP, Brasil
{twalesza, fernandasyw, luizhrotta}@gmail.com, nnimai@fct.unesp.br

[2] Departamento de Engenharia Ambiental, Universidade Estadual Paulista – Unesp/ICT
Rod. Presidente Dutra, Km 137,8, - 12247-004 - São José dos Campos, SP, Brasil
enner.alcantara@ict.unesp.br

Abstract. Water clarity can be considered as the key information to assess water quality. This information can be related to the vertical visibility, analogous to the Secchi disk depth ($\boldsymbol{Z_{SD}}$), which is measured manually with a Secchi disk or by remote sensing. The second one uses bio-optical models, however, most of them were calibrated for oceanic and coastal waters. The semi-analytical approach uses as input, the inherent optical properties (IOPs) retrieved from the quasi-analytical algorithm (QAA) designed for seawaters. Therefore, we hypothesized that error caused by the use of a semi-analytical designed for oceanic waters will prevent an accurately $\boldsymbol{Z_{SD}}$ estimation in an oligo-to-mesotrophic reservoir. Aiming to test this hypothesis, we used *in situ* data collected in three different dates considering OLI/Landsat-8 bands. As result, we noticed that according to the reservoir optical water quality, the estimation of $\boldsymbol{Z_{SD}}$ returned Mean Absolute Percentage Errors ranging between 12.23% and 28.10% when compared to *in situ* data. We also used a dataset (n = 6) collected two and three days before OLI's overpass in order to validate the model using satellite data and the errors were 9.18% and 6.32% for the 2 and 3-day delay, respectively. These results showed that QAA designed for seawaters was able to retrieve $\boldsymbol{Z_{SD}}$ in an oligo-to-mesotrophic reservoir, probably because the closed bio-optical properties from both environments, assuming to be applicable to water clarity monitoring.

Palavras-chave: remote sensing, water quality, inland water, optical properties, sensoriamento remoto, qualidade da água, águas interiores, propriedades óticas.

1. Introduction

The attenuation of light with depth is dictated by water molecules, phytoplankton productivity, particulate and dissolved matter distribution and can be described by the vertical attenuation coefficient, K_d (m^{-1}) and the beam attenuation coefficient, c (m^{-1}) (Kirk 1975). The vertical visibility, analogous to the Secchi disk depth (Z_{SD}), is very common and an easy way to measure light attenuation in the vertical direction as well as trophic state of a water body. Many efforts have been done in order to estimate Z_{SD} considering oceanic, coastal and inland waters (Buiteveld 1995; Doron et al. 2007; Lee et al. 2015; Majozi et al. 2014).

Empirical and semi-analytical approaches were carried out aiming to derive K_d and then relate to Z_{SD}, however, all the models were focused on seawater properties; therefore, the optical water quality is different from that found in inland waters with high absorption coefficients. Buiteveld (1995) showed a semi-analytical way to model Z_{SD} and diffuse attenuation of Photosynthetically Active Radiation (PAR), K_{PAR}, using data from four eutrophic lakes in Netherlands. Recent studies showed good results of emipirical Z_{SD} based model in inland waters (Majozi et al. 2014).

In order to avoid aditional calibration and site-specific limitation, the semi-analytical model from Lee et al. (2015) came up with a new reformulation approach to derive Z_{SD} relying only on K_d at a wavelength representing the maximum transparency. This new model

was validated using a large dataset covering different optical environments such as oceanic, coastal and lake waters. As input, the inherent optical properties (IOPs) were used and predicted through the quasi-analytical algorithm (QAA). The main issue regarding this method is that it was based on oceanic and coastal waters (Lee et al. 2002) and some authors have highlighted important liminations of QAA for applications in inland waters.

We hypothesized that since the Z_{SD} model form Lee et al. (2016) uses the QAA version 5 to estimate the total absorption coefficient, a, and the backscattering coefficient, b_b, in order to estimate the K_d and then the Z_{SD}, the error caused by these estimation will prevent an accuretelly Z_{SD} estimation in a oligo-to-mesotrophic reservoir. To test this hypothesis, data collected in three field trips were used in order to apply the Z_{SD} model considering the spectral bands from Operational Land Imager (OLI)/Landsat-8. Then, the aim of this work was to validate the Z_{SD} model for inland waters with trophic status varying from oligo-to-mesotrophic conditions.

2. Materials and Methods

2.1 Study Area

Nav is a run-of-river reservoir (Figure 1) with a mean water level fluctuation lower than 0.50 m.year^{-1} and is also the fifth of six reservoirs situated along the Tietê River in the west region of São Paulo State, Brazil and started its activity in 1982 flooding an area of 210 km² (at its maximum quota), with a usable volume of 3.8×10^8 m^3, perimeter of 462 km, maximum depth of 30 m, mean residence time of water of about 46 days and an average flow of 688 m^3.s^{-1} (Torloni et al. 1993).

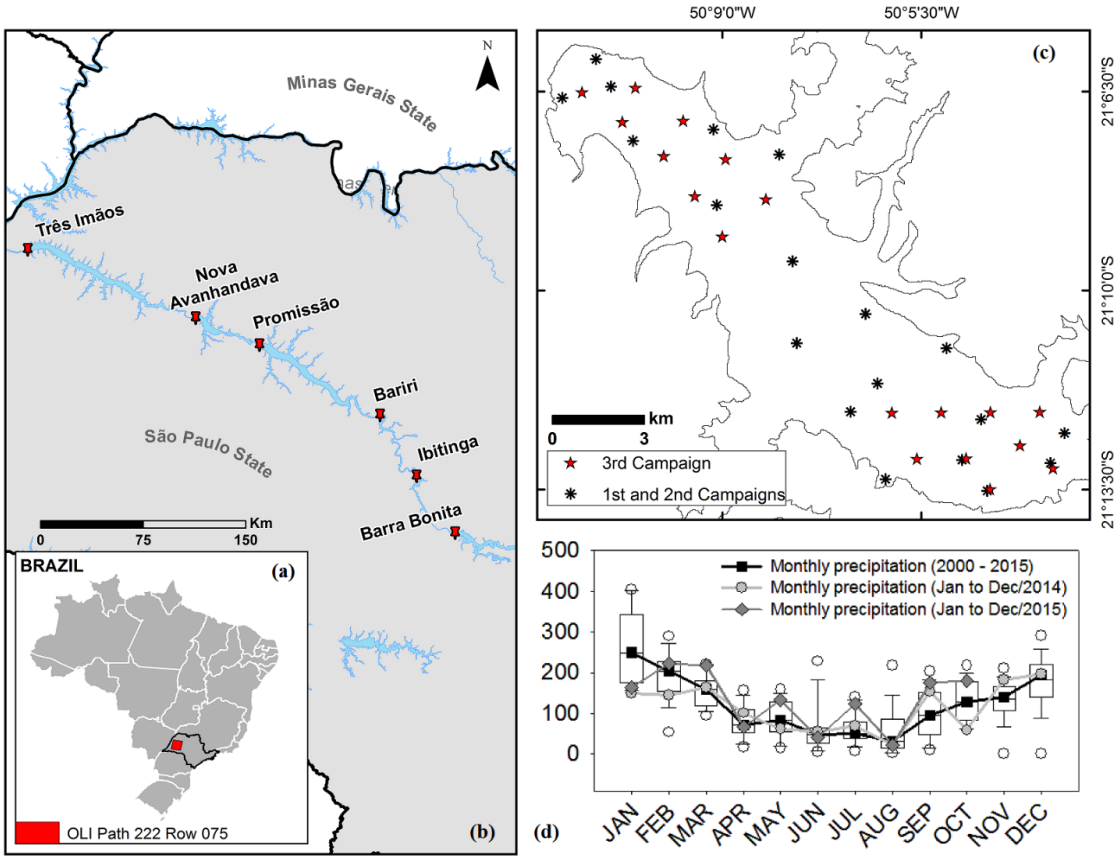


Figure 1. Maps of the study area emphasizing (a) the territory of Brazil highlighted by the OLI/Landsat-8 tile, (b) the State of São Paulo and the respective reservoirs along the Tietê River starting with Barra Bonita, the first of the cascade followed by the downstream reservoirs of Ibitinga, Bariri, Promissão, Nova Avanhandava and Três Irmãos, (c) the sampling location in Nav reservoir and (d) monthly rainfall data from NASA's GIOVANNI

database for the period of 2000 – 2015.

2.2 Laboratory Analysis

The field trips were carried out in the dry (Austral Autumn, April 28 to May 2) and wet seasons (Austral Spring September 23 to 26) of 2014 and the dry season (Austral Autumn, May 9 and 14) of 2016. The first and second field collections resulted in 19 data points each, and 18 for the third one (see Figure 1 for sampling stations location). The chlorophyll-*a* (chl-*a*) was extracted with 90% acetone solution and analyzed spectrophotometrically at 663 and 750 nm (Golterman et al. 1978). The total suspended solid (TSS) concentration was determined through the method described by APHA (1998). A Secchi disk with a diameter of 30 cm was used for Z_{SD} measurements. To estimate the CDOM absorption coefficient (a_{CDOM}), the method from Tilstone et al. (2002) was used and to derive the total particulate absorption coefficient (a_p), non-algal particle coefficient (a_{NAP}) and the phytoplankton absorption coefficient (a_ϕ), Tassan and Ferrari (1995, 1998) approaches were applied.

2.3 In-situ Radiometric Data

The remote sensing reflectance (R_{rs}, sr^{-1}) spectrum was estimated from radiometric measurements taken at each sample station. Below and above water radiometric measurements were acquired using hyperspectral radiometers RAMSES TriOS® (TriOS, Germany) operating in the spectral range between 400 and 900 nm. The acquisition geometry follows the protocol described by Mueller (2000) and Mobley (1999) and aimed to meet requirements to avoid the effects of radiance and specular boat shading. The R_{rs} values were calculated from the radiometric quantities collected in the water surface in accordance with Mobley (1999) (Equation 1):

$$R_{rs}(\lambda) = \frac{L_t(\lambda) - \rho L_s(\lambda)}{E_d(\lambda)} \quad (1)$$

where ρ is the proportionality factor that considerer the wind speed, sky radiance distribution, directions seen by the sensor and reflected by the water target. The value applied was 0.028 once the average wind speed did not exceed 5 m.s^{-1} during data collection and the geometry of acquisition was kept the same as Mobley (1999).

The R_{rs} is the main input data for models to retrieve optically significant constituent (OSCs) concentration. However, it is necessary to match the hyperspectral data with those from satellite data by convoluting the spectral response functions of Operational Land Imager (OLI) from Landsat-8 bands to derive the band-weighted reflectance data (Gordon 1995) (Equation 2):

$$R_{rs}^{OLI}(\lambda_k) = \frac{\int_{\lambda_i}^{\lambda_j} S(\lambda) R_{rs}(\lambda)}{\int_{\lambda_i}^{\lambda_j} S(\lambda)} \quad (2)$$

where R_{rs}^{OLI} stands for the remote sensing reflectance convoluted from OLI spectral bands; λ_i and λ_j are the lower and upper limit of the band λ_k, respectively. *S*(λ) is the spectral response function of the *i*th spectral band of OLI (Barsi et al. 2014).

2.4 Z_{SD} Modeling

The Z_{SD} retrieval has been linked to K_d. Lee et al. (2015) came up with a new theoretical model to interpret Z_{SD} based on $K_d(\lambda)$ (Equation 3):

$$K_d(\lambda) = (1 + m_0 \times \theta_s)a(\lambda) + \left(1 - \gamma \frac{b_{bw}(\lambda)}{b_b(\lambda)}\right) \times m_1 \times \left(1 - m_2 \times e^{-m_3 \times a(\lambda)}\right) b_b(\lambda) \quad (3)$$

where m_{0-3} and γ are equal to 0.005, 4.26, 0.52, 10.8 and 0.265, respectively. Z_{SD} is then retrieved as Lee et al. (2015) (Equation 4):

$$Z_{SD_{L15}} = \frac{1}{2.5Min(K_d^{tr})} \ln\left(\frac{|0.14 - R_{rs}^{tr}|}{0.013}\right) \quad (4)$$

where K_d^{tr} is the diffuse attenuation coefficient of downwelling irradiance in the spectral transparent window and here represents the minimum value within the visible domain (443 – 665 nm) and R_{rs}^{tr} represents the remote sensing reflectance of this wavelength.

2.5 Estimating IOPs from QAA

The QAA approach was initially designed to estimate the IOPs in clear waters, assuming an $a(440) < 0.3\ m^{-1}$ (Lee et al., 2002). Since then, modifications were carried out in order to better describe particularities of inland waters, such as those from Le et al. (2009), Yang et al. (2013) and Mishra et al. (2014) using as reference wavelength (λ_0) the band closed to 708 nm. However, these inland waters were classified as eutrophic to hipereutrophic with $a(440) \gg 0.3\ m^{-1}$, such as the QAA from Mishra et al. (2014), designed for a very turbid cyanobacteria-dominated water with $a_\phi(443)$ ranging between 3.44 and 47.21 m^{-1} representing more than 54% of the $a(443)$. Therefore, the former approach was not tested, only QAA from Lee et al. (2009) and here called as QAA_{v5} using bands from OLI/Landsat-8 and with slight modifications in the following two steps (Equations 5 and 6):

$$\chi = \log\left(\frac{0.01 \times r_{rs}(coastal) + r_{rs}(blue)}{r_{rs}(\lambda_0) + 0.005 \times \frac{r_{rs}(red)}{r_{rs}(blue)} \times r_{rs}(red)}\right) \quad (5)$$

$$\eta = 2.2\left\{1 - 1.2\exp\left[-0.9\frac{r_{rs}(coastal)}{r_{rs}(green)}\right]\right\} \quad (6)$$

2.6 OLI/Landsat-8 Atmospheric Correction

Application of imagery data to retrieve information of water bodies requires high quality atmospheric correction. Classical methods such as FLAASH (Fast Line-of-sight Atmospheric Analysis of Hypercubes) were tested due to their simplicity of use and reasonable success in retrieving OSC in inland waters. Besides, the ACOLITE, which is an atmospheric correction and processor for the OLI/Landsat-8 data, was also evaluated. Recently, the Provisional Landsat 8 Surface Reflectance (L8SR) product, which is produced using specialized software and acquired through the Earth Explorer on demand service, has been applied in aquatic environments to retrieve water quality parameters (Concha and Schott 2016).

2.7 Accuracy Assessment

To retrieve Z_{SD} values in Nav, the semi-analytical approach described by Lee et al. (2015) was used and as input, the simulated R_{rs} from OLI/Landsat-8 was also applied. Once the main goal was to verify the accuracy of the original model for retrieving Z_{SD} in inland water such as Nav, which is an oligo-to-mesotrophic reservoir, data from three field trips were used. In order to validate the model based on satellite data, six samples from the first field campaign (collected on 1 and 2 May 2014) were used to extract the values from the atmospherically corrected data, acquired on 4 May 2014 (Path 222, Row 075). The statistical indicators used for validation were the total root mean square difference (RMSD), the mean absolute percentage error (MAPE), and bias (Equations 7, 8 and 9, respectively).

$$RMSD = \sqrt{\frac{1}{n}\sum_{i=1}^{n}\left(x_{est,i} - x_{meas,i}\right)^2} \quad (7)$$

$$MAPE = \frac{100\%}{n}\sum_{i=1}^{n}\left|\frac{x_{est,i} - x_{meas,i}}{x_{meas,i}}\right| \quad (8)$$

$$bias = \frac{1}{n}\sum_{i=1}^{n}\left(x_{est,i} - x_{meas,i}\right) \quad (9)$$

where n is the number of samples, $x_{est,i}$ and $x_{meas,i}$ represent the estimated and measured values, respectively.

3. Results and Discussion

3.1 Biogeochemical and Optical Characterization

The water quality parameters are displayed in Table 1 and it shows how homogenous are the data except when compared with those from the third field trip. The data from 2014 did not show statistical differences from Autumn to Spring exhibiting a seasonal independence. However, data from 2016 showed a statistical change indicating the influence of the rainfall condition (see Figure 1d for rainfall data). The TSS and chl-*a* concentrations from all the field trips are peculiar of an oligo-mesotrophic environment. These results imply that some factor led to the differentiation of water quality properties from 2014 to 2016 and according to Coelho et al. (2015), the southeast of Brazil experienced a major drought event in 2014, affecting the water quality and water availability in this region. In 2016, the precipitation rate turned back to normal providing the increase of surface runoff and therefore the input of sediment loads into the reservoir.

Table 1. Descriptive statistic from the three field trips carried out in Nav (the notations in the table stand for: Aver: average, SD: standard deviation, Min-Max: minimum-maximum).

		Nav 1 (*n* = 19)	**Nav 2 (*n* = 19)**	**Nav 3 (*n* = 18)**
TSS (mg l^{-1})	Aver ± SD	1.00 ± 0.64*	1.00 ± 0.58	2.83 ± 0.65**
	Min-Max	0.10 – 2.60*	0.50 – 2.80	1.87 – 3.67**
chl-a (µg l-1)	Aver ± SD	6.30 ± 2.53	9.01 ± 4.21	26.56 ± 7.03**
	Min-Max	2.46 – 12.56	4.51 – 20.48	15.84 – 38.59**
Turbidity (NTU)	Aver ± SD	1.63 ± 0.42	1.73 ± 0.41	-
	Min-Max	1.01 – 2.47	1.01 – 2.56	-
Z_{SD} (m)	Aver ± SD	3.19 ± 0.62	3.41 ± 0.62	2.97 ± 0.63
	Min-Max	2.29 – 4.80	2.45 – 4.65	1.91 – 3.80
$a(443)$ (m^{-1})	Aver ± SD	0.75 ± 0.12	0.80 ± 0.22	0.99 ± 0.18
	Min-Max	0.49 – 1.06	0.42 – 1.45	0.65 – 1.37
$a_\phi(443)$ (m^{-1})	Aver ± SD	0.17 ± 0.07	0.24 ± 0.09	0.29 ± 0.13
	Min-Max	0.10 – 0.38	0.10 – 0.43	0.11 – 0.57

* n = 16, ** n = 09

The IOPs provide information about the contribution and dominance of certain OSC in the water and can also assist in the estimation of these components using proper algorithms (Mishra et al. 2014; Riddick et al. 2015). At 443 and 560 nm the NAP dominated the total absorption coefficient except the water component (a_{t-w}) in the first field trip with 42.90 ± 6.51% and 48.69 ± 7.61 %, respectively and at 655 nm the phytoplankton contributed with 44.18 ± 9.91 % (Figure 2).

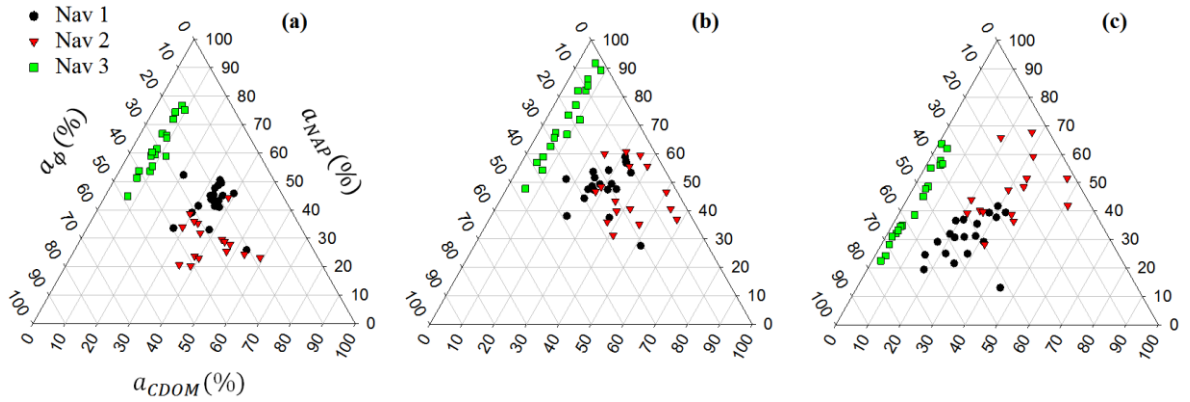


Figure 2. Ternary graphs depicting the absorption budget at three wavelengths in the visible region (a) blue – 443 nm, (b) green – 560 nm and (c) red – 655 nm.

Regarding the second field trip, CDOM contributed with 40.44 ± 8.39 % at 443 nm, followed by NAP with 46.00 ± 9.68 % at 560 nm and 46.88 ± 10.69 % at 655 nm. The third field trip had NAP dominating the blue and green wavelengths with 62.74 ± 9.31 % and 71.68 ± 13.13 %, respectively. At 655 nm the phytoplankton participated with 53.86 ± 13.67 % of the total absorption budget. At 443 nm, the samples were spread within the central zone of the ternary plot indicating that all three absorption coefficients co-varied somehow. The first and third field trips presented the predominance of a_ϕ at 655 nm, which is considered a typical diagnostic feature of phytoplankton and is also attributed to backscattering by CDOM (Gitelson 1992). At all wavelengths, the third field trip presented low percentage contribution of CDOM (less than 10%).

3.2 Atmospheric Correction Assessment

The methods showed different performances considering the coastal to red wavelengths. FLAASH achieved the best result for coastal and green bands with MAPE = 26.49% and 34.12%, respectively while ACOLITE was better for blue and red bands (13.71% and 15.87%, respectively). L8SR showed consistent results (Figure 3a) with MAPE ranging between 54.38% (coastal band) and 27.58% (green band). The latter model was picked because ACOLITE error at coastal band was very high (108.84%) invalidating its use. The comparison between FLAASH and L8SR showed better results for the second one. The method was also used in studies of water quality in inland waters showing good outcomes in terms of spatial modeling of water quality parameters (Concha and Schott 2016). Therefore, this product was elected to display spatially the Z_{SD} values.

3.3 Z_{SD} Algorithm Accuracy and Validation Using OLI/Landsat-8 Data

In order to check the performance of Z_{SD}, R_{rs} data from three different dates were used as input. The IOPs were analytically derived from QAA_{v5} and further applied to retrieve the Z_{SD}. Figure 3(b) showed that values from Nav 1 and Nav 3 were close to the 1:1 line showing a good agreement between *in situ* and estimated values, on the other hand, the values from Nav 2 were underestimated increasing the mean error. The errors were also low for those two field campaigns (Nav 1: RMSD = 0.59 m, MAPE = 13.58% and bias = -0.38 m; Nav 3: RMSD = 0.52 m, MAPE = 12.23% and bias = -0.27 m), however, higher in Nav 2 (RMSD = 0.95 m, MAPE = 28.10% and bias = -0.91 m).

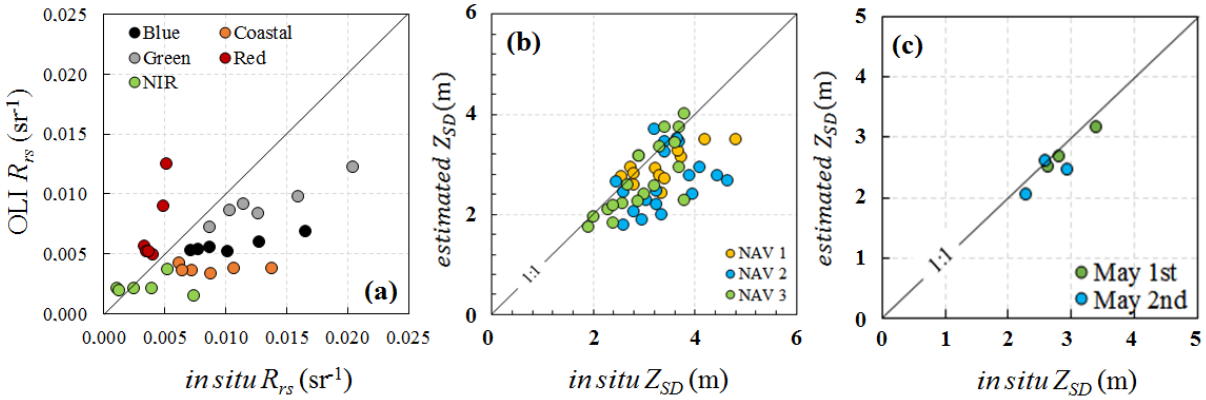


Figure 3. Comparison between estimated and *in situ* Z_{SD} values using: (a) QAA_{v5} and OLI bands, (b) QAA_{M14} and MSI bands, the red arrow indicates the outlier and (c) comparison between estimated and *in situ* Z_{SD} values.

Samples from the first campaign (n = 6) were separated from the whole dataset in order to validate the extracted image data. The semi-analytical model based on surface reflectance OLI product (Figure 3c) showed to be suitable to retrieve Z_{SD} values once the highest uncertainty was found with the 2-day delay data (n = 3) with MAPE = 9.18%, RMSD = 0.32 m and bias = 0.06 m, while for 3-day delay samples (n = 3) the errors had MAPE = 6.32%, RMSD = 0.19 m and bias = -0.06 m. The *in situ* and derived Z_{SD} were positioned close to the 1:1 line, indicating the accomplishment of the model in retrieving Z_{SD} values in an oligo-to-mesotrophic reservoir such as Nav using OLI products. The results showed that this approach can be successfully used in the monitoring of water quality in this type of environment using orbital data with a temporal resolution of 16 days.

4. Final Considerations

A semi analytical model developed to estimate Z_{SD} was evaluated in Nav using simulated OLI/Landsat-8 bands from three field trips carried out in 2014 and 2016. For validation, OLI image-based Z_{SD} was compared with *in situ* Z_{SD} and a good relationship was observed, strongly suggesting the use of OLI/Landsat-8 data to map water clarity in an oligo-to-mesotrophic reservoir. The QAA_{v5} outperformed presenting errors ranging between 12.23% to 28.10%. Taking into account that Nav is not a traditional productive turbid water but an oligo-to-mesotrophic environment with very low TSS and chl-*a* concentrations, the bio-optical properties are very close to that found in oceanic and coastal waters in which the QAA was developed, that is why the success of QAA_{v5}. Therefore, the Z_{SD} showed to be applicable to water clarity monitoring considering Nav's water quality properties.

Acknowledgment

The authors thank to São Paulo Research Foundation - FAPESP (Projects numbers: 2012/19821-1 and 2015/21586-9) and National Counsel of Technological and Scientific Development - CNPq (Projects numbers: 400881/2013-6 and 472131/2012-5) for financial support.

References

APHA/AWWA/WEF. **Standard methods for the examination of water and wastewater**. Washington, DC, 1998.

Barsi, J., Lee, K., Kvaran, G., Markham, B., Pedelty, J. The spectral response of the landsat-8 operational land imager. **Remote Sensing**, v.6, p. 10232–10251, 2014.

Buiteveld, H. A model for calculation of diffuse light attenuation (PAR) and secchi depth. **Netherlands Journal of Aquatic Ecology**, v. 29, n. 1, p. 55–65, 1995.

Coelho, C.A.S, Denis, H.F.C., Firpo, M.A.F. Precipitation Diagnostics of an Exceptionally Dry Event in São Paulo, Brazil. **Theoretical and Applied Climatology**, p. 1–16, 2015.

Concha, J.A.; Schott, J.R. Retrieval of color producing agents in Case 2 waters using Landsat 8. **Remote Sensing of Environment**, v. 185, p. 95–107, 2016.

Doron, M., Babin, M., Mangin, A., Hembise, O. Estimation of Light Penetration, and Horizontal and Vertical Visibility in Oceanic and Coastal Waters from Surface Reflectance. **Journal of Geophysical Research: Oceans**, v. 112, p. 1–15, 2007.

Gitelson, A. The Peak near 700 Nm on Radiance Spectra of Algae and Water: Relationships of Its Magnitude and Position with Chlorophyll Concentration. **International Journal of Remote Sensing**, v. 13, n. 17, p. 3367–73, 1992.

Golterman, H.L., Clymo, R.S., Ohnstad, M.A.M. **Methods for physical and chemical analysis of freshwater**. Oxford: Blackwell Scientific Publications, 1978. 213 p.

Gordon, H.R. A Methodology for Dealing with Broad Spectral. **Applied Optics**, v. 34, n. 36, p. 8363–74, 1995.

Kirk, J.T.O. A theoretical analysis of the contribution of algal cells to the attenuation of light within natural. **New Phytologist**, v. 75, n. 1, p. 11–20, 1975.

Le, C.F., Li, Y.M., Zha, Y., Sun, D., Yin, B. Validation of a Quasi-Analytical Algorithm for Highly Turbid Eutrophic Water of Meiliang Bay in Taihu Lake, China. **IEEE Transactions on Geoscience and Remote Sensing**, v. 47, n. 8, p. 2492–2500, 2009.

Lee, ZP, Carder, K.L., Arnone, R.A. Deriving Inherent Optical Properties from Water Color: A Multiband Quasi-Analytical Algorithm for Optically Deep Waters. **Applied Optics**, v. 41, n. 27, p. 5755–5772, 2002.

Lee, ZP., Lubac, B., Werdell, J., Arnone, R. An **Update of the Quasi-Analytical Algorithm (QAA_v5)**, 2009. Disponível em: < http://www.ioccg.org/groups/Software_OCA/QAA_v5.pdf >. Acesso em: 12.mar. 2015.

Lee, ZP, Shang, S., Hu, C., Du, K., Weidemann, A., Hou, W., Lin, J., Lin, G. Secchi Disk Depth: A New Theory and Mechanistic Model for Underwater Visibility. **Remote Sensing of Environment**, v. 169, p. 139–49, 2015.

Lee, ZP, Shang, S., Qi, L., Yan, J., Lin, G. A Semi-Analytical Scheme to Estimate Secchi-Disk Depth from Landsat-8 Measurements. **Remote Sensing of Environment**, v. 177, p. 101–106, 2016.

Majozi, N.P., Suhyb, M., Bernard, S., Harper, D.M., Ghirmai, M. Remote Sensing of Environment Remote Sensing of Euphotic Depth in Shallow Tropical Inland Waters of Lake Naivasha Using MERIS Data. **Remote Sensing of Environment,** v. 148, p. 178–89, 2014.

Mobley, C.D. Estimation of the Remote-Sensing Reflectance from above-Surface Measurements. **Applied Optics,** v. 38, n. 36, p. 7442–55, 1999.

Mishra, S., Mishra, D.R., Lee, ZP. Bio-Optical Inversion in Highly Turbid and Cyanobacteria-Dominated Waters. **IEEE Transactions on Geoscience and Remote Sensing**, v. 52, n. 1, p. 375–88, 2014.

Mueller, J.L. **In-water radiometric profile measurements and data analysis protocols**. In: Fargion, G. S., Mueller, J. L., (Eds.), Ocean Optics Protocols for Satellite Ocean Color Sensor Validation, Goddard Space Flight Center, Greenbelt, Maryland, NASA Tech. Memo. 2000209966/Rev2 1, 2000. p. 87–97.

Riddick, C.A.L., Hunter, P.D., Tyler, A.N., Vicente, V.M., Horváth, H., Kovács, A.W., Preston, L.V.T., Presing, M. Spatial Variability of Absorption Coefficients over a Biogeochemical Gradient in a Large and Optically Complex Shallow Lake. **Journal of Geophysical Research: Oceans**, v. 120, n. 10, p. 7040–66, 2015.

Tassan, S.; Ferrari, G.M. An alternative approach to absorption measurements of aquatic particles retained on filters. **Limnology and Oceanography**, v. 40, n. 8, p. 1358-1368, 1995.

Tassan, S.; Ferrari, G.M. Measurement of light absorption by aquatic particles retained on filters: determination of the optical pathlength amplification by the 'transmittance-reflectance' method. **Journal of Plankton Research**, v. 20, n. 9, p. 1699-1709, 1998.

Tilstone, G., Moore, G.F., Sorensen, K., Doerffer, R., Rottgers, R., Ruddick, K.G., Pasterkamp, R., Jorgensen, P.V. **REVAMP, Regional Validation of MERIS Chlorophyll products in North Sea coastal waters, protocols**. European Union FPV: EVG1 CT 2001 00049, 2002. 68 p.

Torloni, C.E.C., Corrêa, A.R.A., Carvalho Jr., A.A., Santos, J.J., Gonçalves, J.L., Gereto, E.J., Cruz, J.A., Moreira, J.A., Silva, D.C., Deus, E.F., Ferreira, A.S. **Produção pesqueira e composição das capturas em reservatórios sob concessão da CESP nos rios Tietê, Paraná e Grande, no período de 1986 a 1991**. São Paulo: CESP, 1993. 73 p.

Yang, W., Matsushita, B., Chen, J., Yoshimura, K., Fukushima, T. Retrieval of Inherent Optical Properties for Turbid Inland Waters From Remote-Sensing Reflectance. **IEEE Transactions on Geoscience and Remote Sensing**, v. 51, n. 6, p. 3761–73, 2013.